IOSR Journal of Mechanical and Civil Engineering (IOSR-JMCE)
e-ISSN: 2278-1684,p-ISSN: 2320-334X, Volume 18, Issue 6 Ser. I (Nov. – Dec. 2021), PP 54-65
www.iosrjournals.org

Aging of Cast Aluminum Alloy A356: Effects on Mechanical Properties and Microstructure

Victor Alcántara Alza[1]
[1](*Mechanics and Energy / National University of Trujillo, Perú*)

Abstract:
The effect of natural and artificial aging treatment on the hardness and mechanical properties of aluminum alloy A-356 was investigated. To measure the hardness, 20mmx30mmx10mm specimens were used and the ASTM E 8M standard was followed for the tensile tests. First, all the samples were solubilized at 540 ° C (12 h), and then they were subjected to three tempering means: Water (+ 80 ° C), Air (23 ° C) and Dry ice (-40 ° C). Then, for the natural aging T4, the holding times were used: 2; 4; 6; 8 and 10 h; and for the artificial aging T6, the specimens were reheated to 150 ° C and the same times were used. It was found; that the hardness for the T4 and T6 treatments are increased by increasing the holding time and the highest values are found when the samples are cooled in dry ice (-40 ° C). For treatment T4 the hardness varies between 80 HV-93 HV, and for treatment T6 the values are between 65 HV -100 HV. Yield strength (YS) and mechanical strength (UTS) increase with artificial aging time and elongation "ε" shows a tendency to embrittle with time. The maximum UTS is 300 MPa, and it is achieved with the longest natural and artificial aging time (10 h). The maximum ductility: ε = 11%, is linked to a UTS of 250 MPa and is achieved with the longest natural aging time (10 h) and the minimum artificial aging time (2 h). All the microstructures show a matrix of the primary phase α, enriched in aluminum and Silicon, surrounded by eutectic structures with different types of precipitates of different morphology and composition; such as: Mg2Si, Al12Mg2Si, Al9Si.

Key Word*: Aluminum alloys; Precipitation; Aging, microstructural evolution, tensile property*

Date of Submission: 12-11-2021 Date of Acceptance: 28-11-2021

I. Introduction

In the automotive industry there is a growing demand to reduce the weight of vehicles, to improve fuel efficiency and control of gas emissions. Aluminum alloys have attracted great attention in these applications due to their excellent molding ability, corrosion resistance and especially their high weight / strength ratio **[1, 2].** These alloys have a density that is approximately one third of steel.

Aluminum alloys can be of two types: wrought or Cast, and all of them are hardened by heat treatment or by deformation. Cast aluminum alloys mainly contain Si, Cu and Mg as the main alloying elements. Copper and Magnesium strengthen the alloy matrix and improve mechanical properties and machinability **[3,4].** Among the most important variables affect the mechanical properties of aluminum casting are: Chemical composition, solidification rate, metal strength and heat treatment **[5].**

In the cast condition, only some Al alloys containing Cu and others containing Mg and Si are heat treatable, due to the precipitation strengthening mechanisms. One of the main families of heat treatable cast aluminum alloys containing magnesium and silicon is the 3xx series. The use of the term "heat treatment" applied to aluminum alloys is restricted to the specific operation intended to increase the mechanical resistance and hardness in aluminum alloys by means of aging or precipitation hardening **[6].** This treatment consists of raising the temperature to a point where the alloying element is completely soluble and after a certain homogenization time, the temperature is quickly lowered by quenching, usually in cold water and leaving it for an adequate time at room temperature. (natural aging) to make the precipitates uniform, and another way would be; after hardening and cooling, the temperature is raised again in a range: 150-180 ° C, where a controlled precipitation of the alloy occurs (artificial aging). Precipitation hardening or aging treatment is an important hardening method used to increase the strength of most aluminum alloys **[7, 8].** Quenching can also be done with hot water or in sub-zero media. Hot water cooling is recommended for alloys 356 and 319 as it minimizes stresses and quenching distortion **[9].** Regarding the solution temperature, the recommendation of Samuel et all., can be considered **[10];** who reported that solution treatment at 500 °C for 8-10 h seemed to be the recommended solution treatment for high Mg alloys (A319).

One of the most versatile cast aluminum alloys in the 3xx series (AI-Si-Mg) is the A356 alloy that has been chosen as the subject of study. It is widely used in high strength components for automotive, aerospace and military applications, due to its excellent cast ability, weldability, high strength, mechanical and corrosion

resistance **[11].** The main components of this alloy are Mg and Si; These alloys possess high mechanical strength due to the Mg2Si phase or intermetallic compound, which is formed during the precipitation hardening or aging treatment. This treatment is carried out in two stages; First, a solution treatment is carried out and after rapid cooling, a natural or artificial aging is applied, which provides growth control and a composition consisting of a matrix rich in aluminum **[12, 13].** However, if there is an excessive growth of these precipitates through treatments at high temperatures or very long times, the movement of dislocations that occur from inconsistencies in the softening of the alloy is facilitated. This treatment is well known as over aging. On the other hand, the volume fraction of Mg2Si is mainly affected by the level of Mg within the alloy; being the content of Si also important.

So far, various investigations have been conducted that have examined the mechanical properties of cast aluminum alloys after T6 treatment. Many of them report having achieved high-strength alloys, from an Al-Si alloy with Cu and Mg contents, through the aging treatment; It was also found that the hardening is due to the precipitation resulting from the intermediate or intermetallic phases of Al_2Cu and Mg_2Si **[14, 15].**

The precipitation sequence during the aging of aluminum alloys goes through several intermediate stages before the precipitates are reached in a state of equilibrium. In Al - Si - Cu - Mg alloys, the precipitation sequences derived from the solid solution are generally the following: Guinier-Preston zones (GP) $\rightarrow\theta'' \rightarrow\theta'$ $\rightarrow\theta$ (Al_2Cu, equilibrium) y zones GP $\rightarrow\beta'' \rightarrow \beta' \rightarrow\beta$ (Mg_2Si, equilibrium) **[16].** The high tensile strength and high ductility obtained for cast aluminum alloys A356 (Al-Si-Mg base alloy) are due to the spheroidization of the Si particles arising from the T6 aging treatment and a consequent reduction in tensions concentration at Si / eutectic interface and matrix interfaces **[17, 18].** The high strength properties have also been attributed to the presence of precipitated spherical GP zones with Mg and Si enrichment; It to say, β′ (Mg_2Si) **[19].**

Serizawa et al **[20],** investigated at the nanoscale level, the precipitated microstructures of Al-Mg-Si wrought aluminum alloy. They found two exothermic peaks within a range of room temperature and 100 ° C. This phenomenon is explained by the formation of two types of Mg-Si nanoclusters, with different Mg / Si ratios. Similar results were found by Ceschini et al **[21]** for cast aluminum alloy A356. The formation of these nanoclusters is of great interest, because it directly influences subsequent precipitation, so that a "pre-aging" at room temperature between quenching and artificial aging can influence the final mechanical properties of the alloy **[21,22].**

According to Edwards et al **[22]** the precipitation sequence is: co-clusters of Si and Mg atoms small precipitates of unknown structure or phase β" → phase β ' + phase B'→phase β. The β " phase is considered the main reinforcing phase in these alloys **[21, 22, 23,].** The chemical composition of these compounds are: β' = $Mg_{1.8}Si$; β"=Mg_5Si_6; β = Mg_2Si. The last sequence of precipitation is influenced by the Si content of the alloy.

S. Hafenstein, and E. Werner **[24],** studied the direct aging process of a hot isostatically pressed A356 aluminum casting alloy, finding that the strength of age-hardenable Al-Si-Mg aluminum alloys can be increased compared to conventionally heat-treated T6 cast alloys, if pre-aging at room temperature is avoided.

M. Gwózdz and K. Kwapisz **[25]** investigated the Influence of the aging process on the microstructure and mechanical properties of molten aluminum and silicon alloys - Al-9% Si-3% Cu and Al - 9% Si - 0.4% Mg. The solidification rate was shown to have a great influence on the mechanical properties, as it controls the microstructure. A peak in yield strength of 197 MPa for Al-Si-Cu alloy and 243 MPa for Al-Si-Mg was reached. concluded that the appropriate adjustment of the artificial aging time is the key factor to obtain superior properties of these alloys; Therefore, it is necessary to adjust it individually for each material due to differences in response of different alloying elements to heat treatment.

It should be take account, the catalogs of the manufacturers of these alloys do not provide specific data to choose an appropriate precipitation treatment and if they do it, is in a very specific way according to the form of manufacture that they use. Therefore, the objective of this research is to find the appropriate conditions for the natural T4 and artificial T6 aging treatments applied to the cast aluminum alloy A356, taking into account a constant solubility temperature of 540 °C and an artificial aging temperature. 150 °C, with immersion times that vary between (0-10h). The results will allow choosing the most suitable treatment conditions for hardening and mechanical resistance of this material for a pre-established industrial application.

II. Material and Methods

The chemical composition of cast aluminum alloy A-356 is shown in table 1. A typical cast aluminum alloy of the Al-Si-Mg type is observed. The other elements can be considered as traces with a small fraction of Fe.

Table.1. Chemical Composition of Aluminum Alloy A-356 (w%).

Si	Mg	Cu	Ti	Pb	Sn	Ni	Fe	Al
6.82	0.35	0.022	0.100	0.013	0.042	0.006	0.11	Bal.

All The test samples were made from pre-cut A356 aluminum coupons. The specimens for hardness tests were machined, in the shape of parallelepipeds of 10 x20mmx30mm. The tensile specimens were manufactured from the same coupons, with different geometry. The specimens for tensile test was manufactured according to the ASTM E8-82 standard, whose sketch is shown in figure 1,

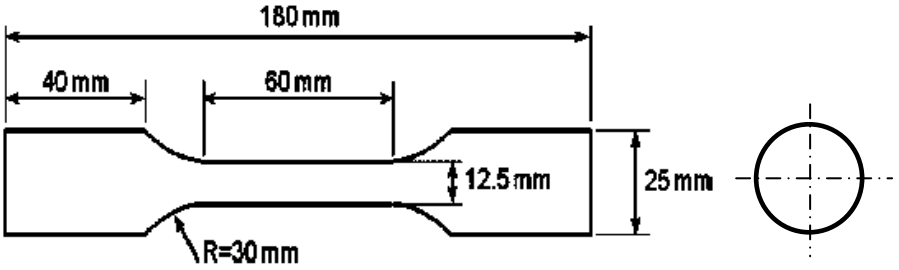

Figure 1. Schematic drawing, to make tensile specimens according to the standard ASTM E8-82

2.1. Heat Treatments Schedule

The heat treatment program, which includes solubility processes; natural and artificial aged. (Treatments T4 and T6) can be seen in figure 2. The solution and aging temperatures have been taken considering the recommendations of the EN-46400 standard.

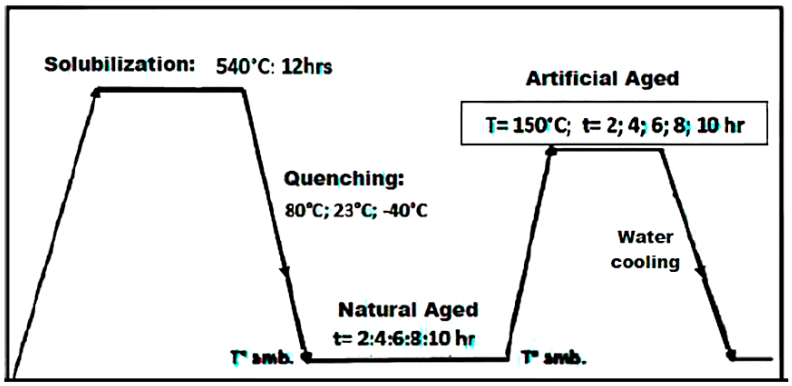

Figure 2, Sequence of heat treatments: 1) Solubilized; 2) Temper with three cooling media; 3) Natural aged at room temperature; 4) Artificially aged at T° = 150 ° C with cooling in water.

2.2. Microhardness Tests.

Microhardness tests were performed on a VICKER HVS-1000 digital microdurometer. The standard was followed: ASTM E384-09, using a load of (176.8 N) with an indentation in a time range: 10-15 s. Before conducting these tests, the specimens were ground and surface polished to ensure measurement. The polishing was carried out with sandpaper: 400, 800 and alumina cloth. Then three (3) measurements were made in each specimen, averaging the results obtained.

2.3. Traction Tests.

The tests were carried out at room temperature in the IMSTRON UNIVERSAL 8801 10 Ton machine, following the ASTM E 8-82 standard. Before being tested, all the specimens were previously rectified and polished. All the tests followed the standard established above. In figure 3 some samples are observed before being tested.

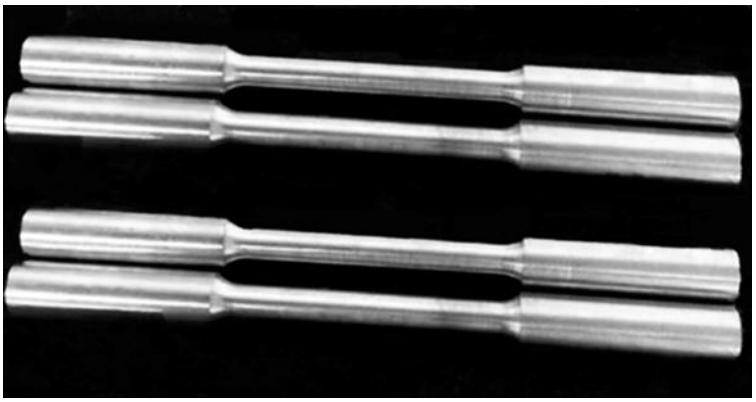

Figure 3. Ground and polished machined specimens; ready for tensile tests.

2.4. Microscopy Test

The microscopy analysis, was done at optical level, using the Zeiss 1000X Microscope. In order to reveal the microstructure, the samples surfaces were roughened, polished and chemically etched. Then they were encapsulated to make a roughing with sandpaper from grade 220 to 1000; then they were polished with a corduroy cloth with alumina from grade 5 µ, 3 µ, 1 µ, to 0.3 µ and water, for 30 sec. Finally, they were attacked with the reagent: Composition hydrofluoric acid: [Hydrofluoric acid 0.5 ml, water: 99.5 ml.], According to recommendations given in reference **[26].**

III. Results

3.1. Microhardness

The results of natural and artificial aging are shown in table 2. The solubilization treatment was carried out at 540 °C, for 12 h. Three quenching media were used in cooling. Then the natural and artificial aging were carried out and cooled to room temperature with the times indicated in table 2. The corresponding graphs are found in figure 4 (a) for natural aging (T4) and figure 4 (b) for artificial aging (T6). In both cases it is observed that the hardness is greater when the temper is more severe; that is, when the tempering is carried out at a lower temperature, a higher cooling rate occurs. More will be discussed later.

Table 2. Microhardness results in cast aluminum A-356 samples subjected to natural aging at room temperature and artificial temperature, T° = 150 °C, with different cooling media and aging times.

Microhardness in Natural Aged Samples (NA)					
Quenching Medium: Hot water (+80 °C)					
Time (h)	2	4	6	8	10
Hardness (Hv)	75,0	85,4	87,3	90	89,3
Quenching Medium: Room temperature (23 °C)					
Time (h)	2	4	6	8	10
Hardness (Hv)	77,2	90,0	92,5	94,2	95,0
Quenching Medium: Dry ice (-40°C)					
Time (h)	2	4	6	8	10
Hardness (Hv)	83,3	96,0	95,3	94,8	95,3
Microhardness in Artificial Aged Samples (AA): [T_{AA} = 150°C]					
Quenching Medium: Hot water (+80 °C)					
Time (h)	2,0	4,0	6,0	8,0	10,0
Hardness (Hv)	62,0	94,0	95,4	94,0	96,5
Quenching Medium: Room temperature (23°C)					
Time (h)	2,0	4,0	6,0	8,0	10,0
Hardness (Hv)	64,0	97,5	98,0	97,7	100
Quenching Medium: Dry ice (-40°C)					
Time (h)	2,0	4,0	6,0	8,0	10,0
Hardness (Hv)	69,0	107,0	106,0	105,0	109,0

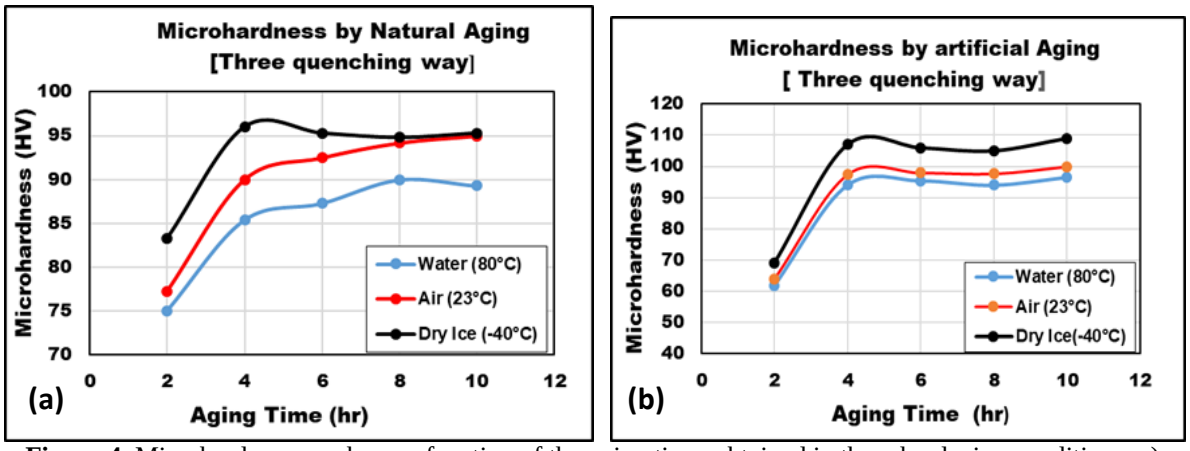

Figure 4. Microhardness graphs as a function of the aging time, obtained in three hardening conditions: a) Microhardnes by Natural Aging; b) Microhardness by Artificial Aging.

3.2. Traction Mechanical Properties

Due to the great variety of data that would be obtained for the three cooling media, only the mechanical properties of the specimens cooled in hot water (+ 80 °C) are shown. For the other media, trends can be induced with the hardness results.

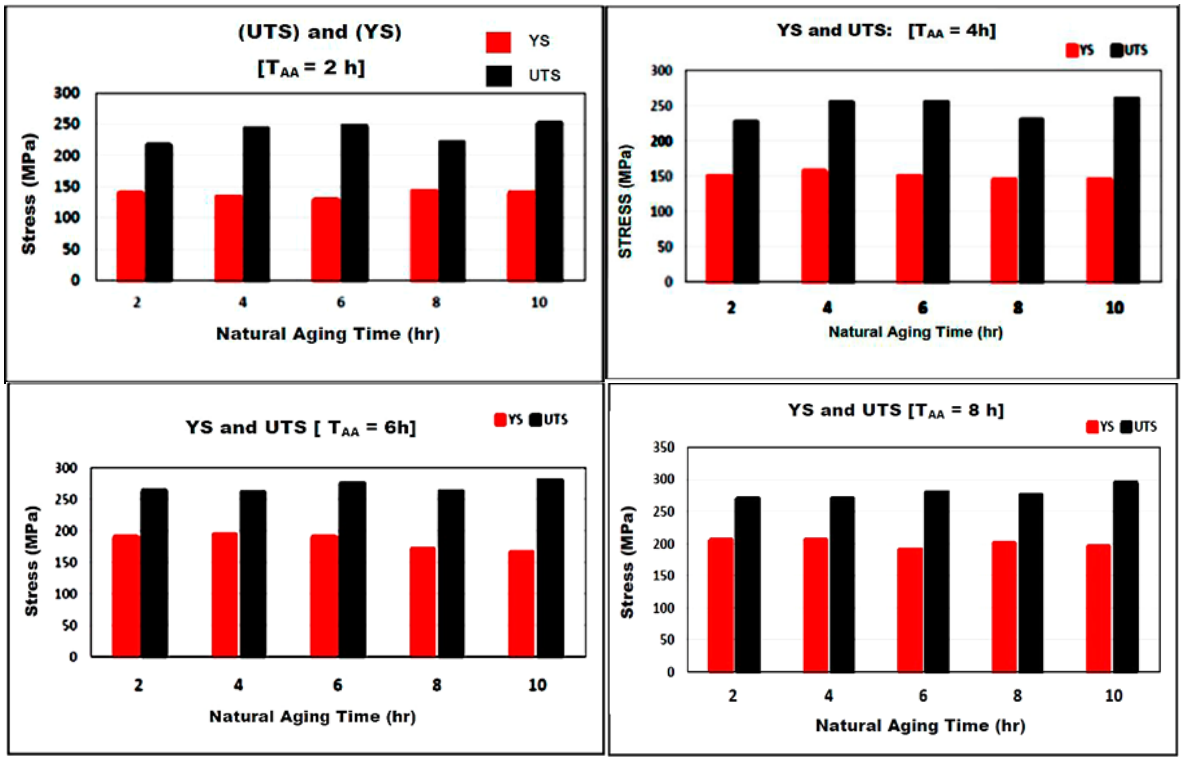

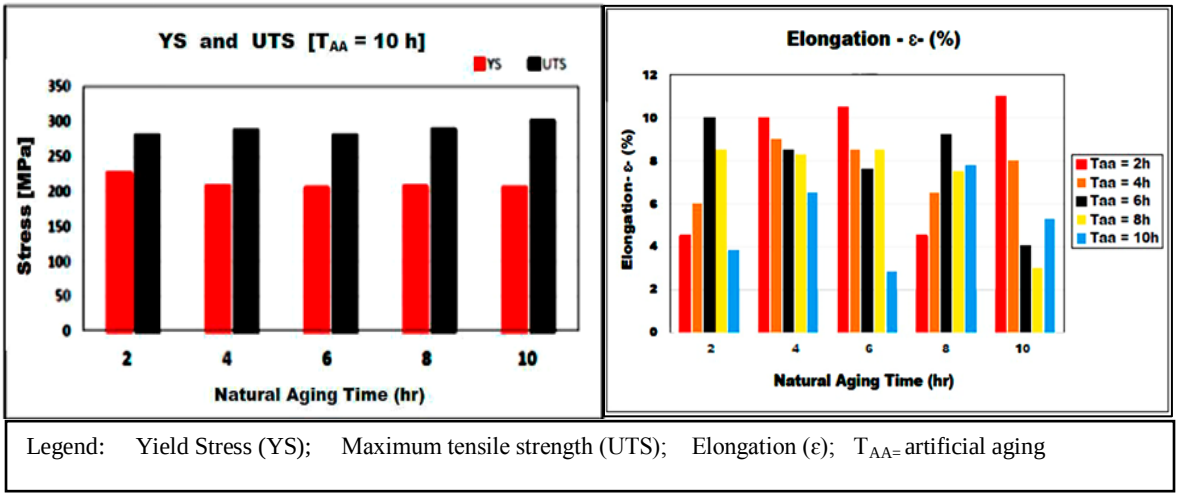

Figure 5. Mechanical properties of Tensile tests for different natural and artificial aging times (T_{AA}). In the elongation graph ε (%); Taa = $T_{AA.}$

If these graphs are compared with the corresponding curves (σ-ε) of figure 6, it is observed that the aging treatment applied to this material has decreased the elongation ε in all cases with respect to the base material; that is, the aging treatment has a tendency to embrittle the samples. Nevertheless; in almost all cases this is offset by the increase in YS and UTS. This phenomenon is closely related to the precipitation mechanisms of natural and artificial aging treatments.

3.2.1. Stress- Strain Graphs: (σ-ε)

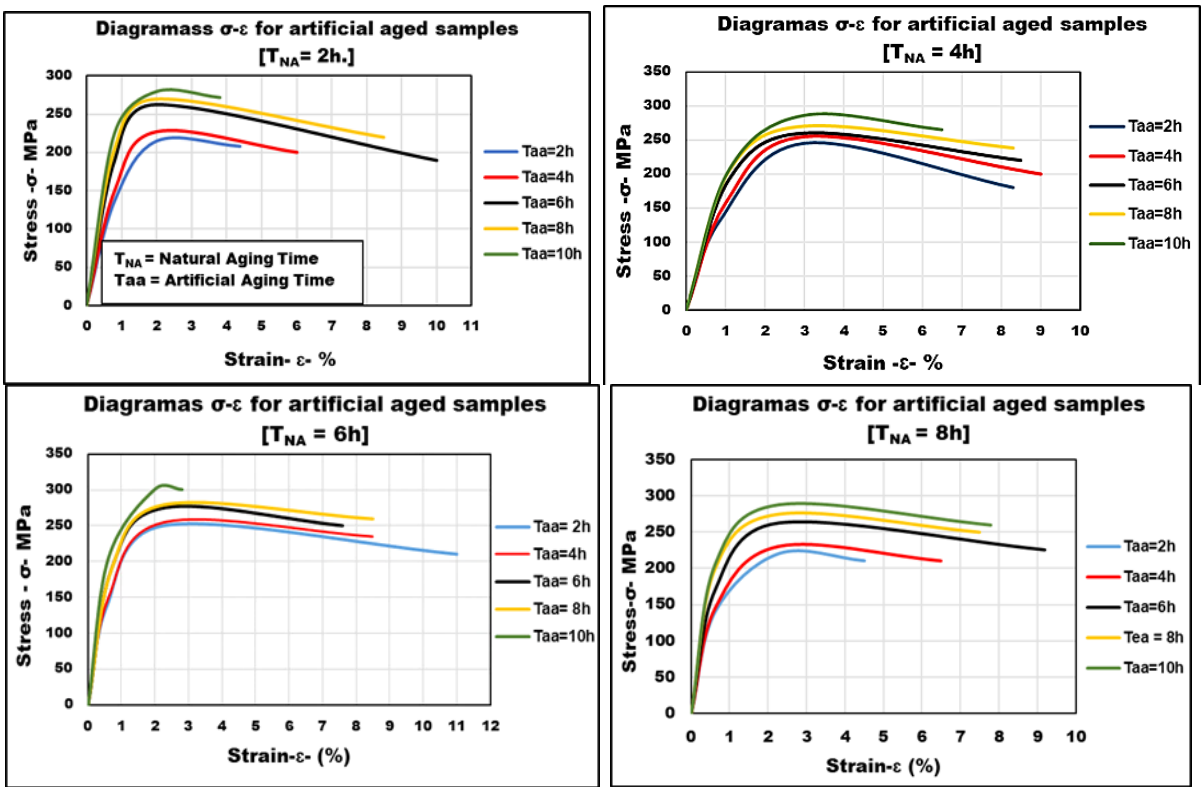

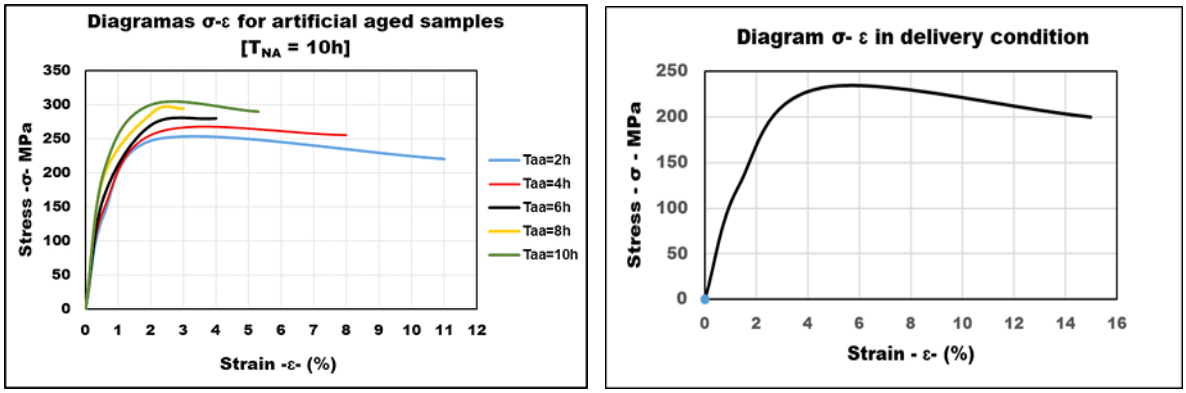

Figure 6. Diagrams (σ-ε) for samples with different natural and artificial aging times. The samples were tempered in hot water (+ 80 °C). The σ-ε curve of the material in the delivery state is included at the end.

3.3. Microstructure:

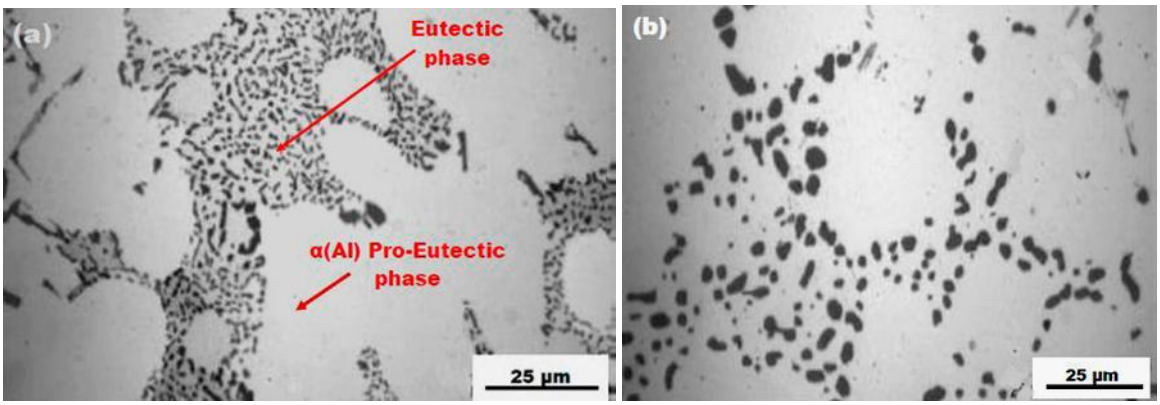

Figure 7. Typical microstructures obtained in an optical microscope for (a) as-cast sample and (b) Solution treated at 540°C on sample of A356 alloy.

3.3.1. Natural Aging Treatment Samples

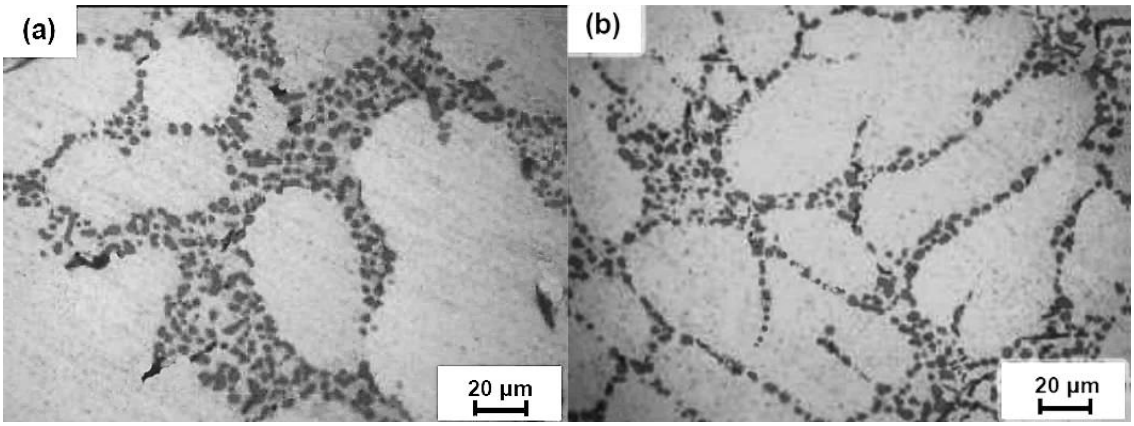

Figure 8. Aged samples with natural aging: a) 2 h b) 4 h.

Figure 7a shows the microstructure of cast aluminum A356 in the delivered state. It is possible to observe the clear zone that corresponds to the zone of proeutectic solution (α) composed of the elements Al, Mg and Si; which is a solution rich in aluminum. In figure 7b) a photomicrograph has been taken of a solubilized sample without it having produced natural aging. The dissolution of the precipitates in the eutectic zone is observed.

In Figure 8a) two photomicrographs taken on the same scale are shown, where the effect of natural aging (T4) is observed. In both cases a transformation of the proeutectic light zone is observed and thicker

precipitates of different morphology are also distinguished in the Eutectic zone (dark zone). It is a situation that has produced changes in hardness and mechanical properties. The microstructure will be discussed in more detail later.

3.3.2. Artificial Aging Treatment Samples

They are observed in figure 9. It should be noted that these come from a quenching in hot water (+80°C).

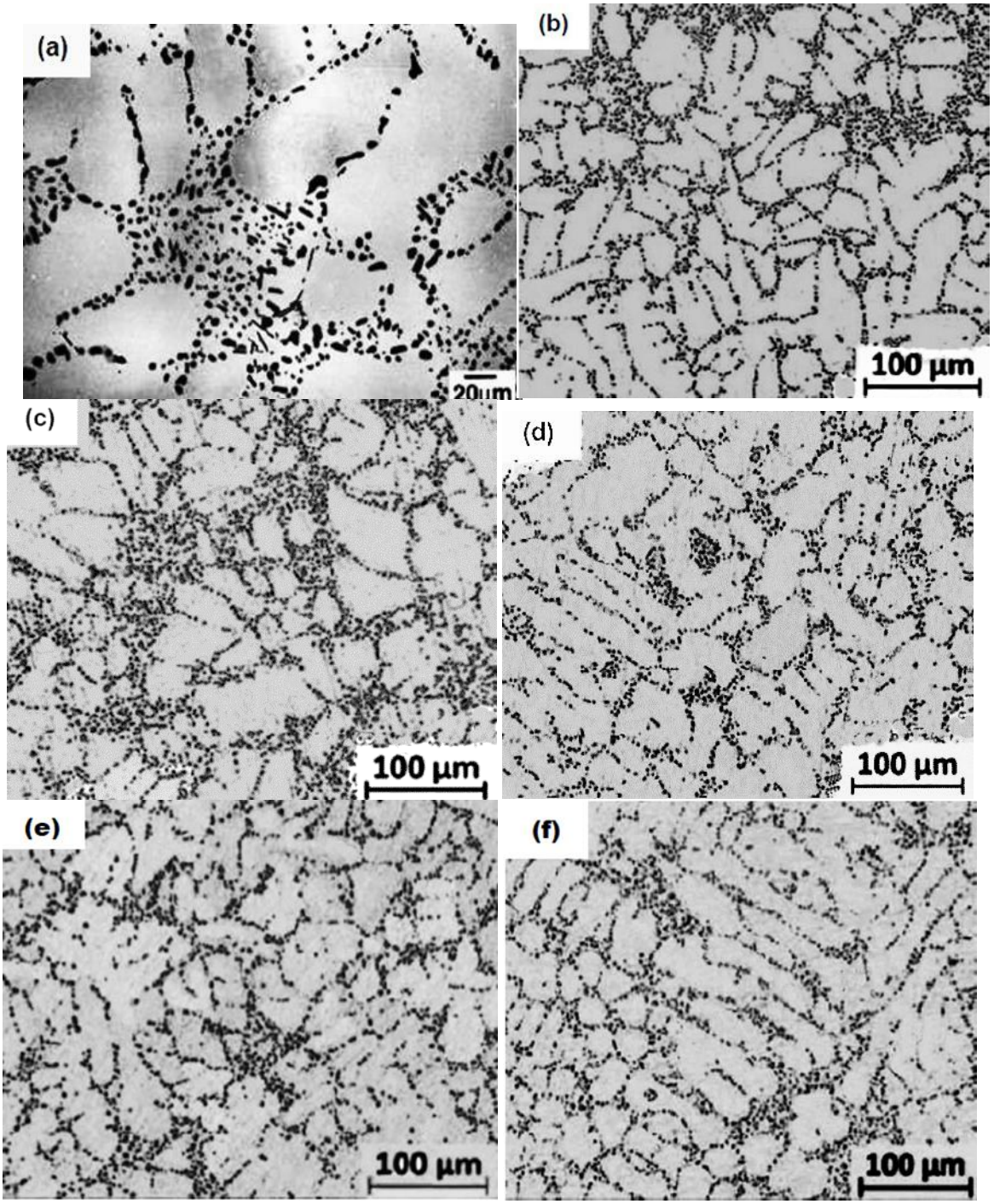

Figure 9. Microstructures of A356 alloy aged at 150 °C for various times of artificial aging, immediately after quenching: (a) Delivery; (b) 2 h; (c) 4 h; (d) 6 h; (e) 8 h; (f) 10 h. The microstructures correspond to samples tempered in hot water (+ 80 °C).

IV. Discussion

4.1. Microhardness with Natural Aging.

In table 2, the hardness results obtained with natural and artificial aging are shown, the quenching having been carried out in three cooling media: water (+80 °C); air (23 °C) and dry ice (-40 °C). The artificial aging was carried out at T ° = 150 °C. Their trend graphs are seen in Figure 4. The trend of the three curves is increasing for the three cooling media and the hardness increases with time due to the precipitating phases, depending on the cooling medium. The graph of figure 4a) indicates: For a constant solubilization time and temperature, the hardness is in direct relation to the natural aging time and the cooling medium; that is to say: "If the quenching is more severe (cooling at lower temperatures), the natural aging hardness is higher regardless of the holding time"; because in some intervals it increases and in others decreases. The general tendency is to increase the hardness. For the first 4 hours of aging, both natural and artificial aging produce a sudden increase in hardness. After this time, the samples with natural aging quenching in dry ice tend to decrease; but in water and air tends to increase. In the artificially aged samples; those that were quenching in dry ice after the first 4 hours, the hardness tends to decrease and the samples with water and air quenching the hardness tends to stabilize.

The maximum hardness value obtained was 109 HV for artificial aging, and 96 HV for natural aging. Both were obtained with a dry ice quenching; having produced an increase of 13.5% due to the high degree of precipitation with artificial aging. The cooling medium in quenching greatly influences the hardness of this type of alloy. This is explained by the fact that a higher cooling rate, there is greater supersaturation and the diffusion rate of the solute decreases as the temperature decreases. When the supersaturation or diffusion rate is low, the precipitation rate is low and viceversa. During this stage of maturation or natural aging, the alloy hardens progressively and spontaneously and the solid solution decomposes to give rise to the formation of small areas or clusters of solute atoms. (Guinier- Preston zones or GP zones). These GP zones introduce elastic distortions into the matrix network. In certain cases, this precipitation is facilitated by the presence of defects in the network, such as dislocations, which favor a higher diffusion of solute atoms **[31].** Then the precipitation of precipitates or intermetallic compounds continues, such as Mg2Si among others, which are responsible for the increase in hardness. **[27].** For this reason, aging treatment is also called precipitation hardening.

4.2. Microhardness with Artificial Aging.

The results are shown in table 2 and their trend graphs are observed in figure 4b). Samples tempered in water (+ 80 °C) show an increasing trend in the interval (2-4h) and then remain almost constant until the end of the interval. The increase has occurred from 62 HV (at the beginning) to 96.5 HV. Samples quenching in air (23 °C) have an increasing tendency until 5 hrs, to later adopt an almost constant value. Samples quenching in dry ice (-40 °C) have an increasing trend until 5 h, then adopt an almost constant value until the end of the interval. The increase has occurred from 69HV to 109HV; which represents an increase of 58% with respect to the initial value. Comparing the graphs, the following is extracted. The three curves have the same tendencies and keep the same relationship as for the previous case (natural aging) with respect to the cooling media. The difference is found in the hardening percentages, which in this case, are higher than for natural aging. On the other hand, the values for the three cases range between 65 HV and 100 HV on average. On the other hand, for natural aging they oscillated between 80 HV and 93HV on average. This shows that the hardening effect is faster in artificial aging.

The notable increase in hardness occurs in the first 4 h, and is in accordance with the work of A. Kelly, R. Nicholson **[28]** who state that during the first aging stages of an Al-Si-Mg alloy (type A356) (155°C /4 h), the saturated solid solution first develops groups of solutes. However, the supersaturation of the vacancies allows diffusion, which leads to the formation of GP zones. These areas of the microstructure are associated with the aging hardening phenomenon, whereby room temperature reactions continue to occur within the material over time, resulting in changing metallurgical and mechanical properties. Physically, GP zones are regions of the material solute-enriched extremely to fine scale or nanometrics, which offer physical obstructions to the movement of dislocations, causing high hardening **[29].** According Edwards et all and C.S.Tsao; The response to aging hardening is attributed to the precipitation of nanometric phases β ″ and / or β ′ inside α (Al) **[22, 32]**

Finally, it can be observed that the hardness values with treatments (T4), decrease in hardness after 5 h. This decrease in hardness is due to the decrease in the concentration of Si in α (Al). Something similar happens with the hardness values obtained with treatment (T6). In this case, the drop in hardness is explained by the fact that the concentration of Mg in α (Al) changes little; giving rise to a small decrease in the concentration of Si in α (Al), and also the Si is distributed in α (Al) in a more homogeneous way **[33].**

4.3. Tensile Mechanical Properties.

Due to the great variety of data obtained, only the mechanical properties of the specimens cooled in hot water (+ 80 °C) are shown. For the other media, trends can be induced with the hardness results. The YS, UTS and "ε" results are plotted as a function of natural and artificial aging time.

For T_{AA} = 2h; the YS values are very close and it could be said that they are almost constant with small oscillations of 127 - 140 MPa whose difference does not exceed 13 MPa. The UTS values have a similar trend with extreme values of 215-250 MPa, the difference of which is 35 MPa. The elongation values "ε" have an increasing trend except for the samples with natural aging of 8h where a pronounced drop is observed, probably due to the appearance of secondary precipitates at this point and then dissolve.

For T_{AA} = 4 h; the YS values are close and not very increasing with values at their extremes of 145-150 MPa whose difference is 5 MPa. The UTS values have a similar trend with extreme values of 227-260 MPa, the difference of which is 33 MPa. The elongation values "ε" show a very irregular trend in their values, with a significant drop at 8 hrs. Probably at this artificial aging temperature a sequence of precipitates of different types appears that would be responsible for this variation.

For T_{AA} = 6 h; YS values are almost constant until 6 h with natural aging, then showing a pronounced drop until 10 h. The extreme values are 193-165 MPa, the difference of which is 28 MPa. The UTS values have an almost constant trend throughout the interval, with extreme values of 260-280 MPa. The elongation "ε" shows decreasing values, where again a drop is observed at 8 h, probably at this artificial aging temperature it is produces a sequence of different types of precipitates that would be responsible for this variation.

For T_{AA} = 8 h; the YS values are almost constant until 6 h, then showing a steep drop at 8 h. The extreme values are 205-190 MPa, whose difference is 15 MPa. The UTS values have an almost similar trend throughout the interval, with extreme values 295-270 MPa, the difference is 25 MPa. The elongation "ε" presents extreme values (8.5-3.0%), with a drastic drop at 10 h.

For T_{AA} = 10 h; the value of YS begins with the highest value in the first 2 h (226 MPa) and then descends to 205 MPa and remains with that value almost constant, until the end of the interval (~ 206 MPa). The extreme values are 226 - 206 MPa with a difference of 20 MPa. The trend of YS is decreasing. On the contrary, the UTS values show an increasing trend with extreme values of 280-300 MPa, with a difference of 20 MPa. The elongation "ε" shows a totally irregular trend.

In Figure 6 the curves (σ-ε) of studied cases of natural and artificial aging can be visualized. These curves synthesize and relate the tensile properties with the natural and artificial aging parameters.

From all the results of the tensile tests, the following is extracted: I) The maximum mechanical resistance UTS is 300 MPa, which is combined with an elongation of 5.3%, and is achieved with the maximum natural and artificial aging time (10 h). II) The maximum ductility ε = 11%, is linked to a UTS value of 250 MPa and is achieved with the maximum natural aging time (10 h) and the minimum artificial aging time (2 h); III) The natural aging process at room temperature before the artificial aging process has a significant impact on the resulting mechanical properties of A356 alloy. Finally, it can be added: In all σ-ε curves, the slopes (straight areas), which determine the elastic limit almost do not vary. That is to say; the modulus of elasticity (E) is almost constant, and does not suffer alteration due a that is a physical property rather than a mechanical onet; effect that is almost general in the majority of the heat treatments in the metals with small limits of variation.

4.4. About the Microstructure.

Figure 7. shows the microstructures obtained at the optical level for (a) freshly melted sample and (b) sample treated with solution for the A356 alloy. In figure 8. The microstructure of the naturally aged samples is shown for: a) 2 h b) 4 h. In figure 9. The A356 alloy microstructures are shown, previously solubilized at 540 ° C (12h) and tempered in water (+ 80 ° C); Then, artificially aged at 150 °C with various holding times: (a) 0h supply; (b) 2 h; (c) 4 h; (d) 6 h; (e) 8 h; (f) 10 h. In all cases the final cooling was in air.

In all the microstructures of figure 9, the clear region is the matrix of the primary phase of aluminum and Silicon, noting the presence of eutectic structures with different types of precipitates and diverse morphology. However, taken together, all microstructures are similar. The α (Al) dendrites and the interdendritic lattice of the Al-Si eutectic phase are easily identified. The Si particles of the eutectic phase show a characteristic globular shape, and no noticeable effect is observed in these microstructures by varying the artificial aging time.

It has not been possible to identify exactly the type of precipitate, but we can make an approximation based on studies of M. Abdulwahab, et al, **[30]** who examined different heat treatments for A356 alloy with various alloy grades. They found the presence of intermetallic phases with various morphologies: Mg_2Si, AlFeSi, $Al_{12}Mg_2Si$, $Al_8Mg_3FeSi_6$, $Al_{12}Si$ (Fe,Cr), Al_3Cr, Al_8Cr5, Al_9Si, $AlFe_4Mg_{17}$. According to the chemical composition of our specific alloy that does not contain Fe or Cr. The probable intermetallic compounds can only be three of them: Mg_2Si, $Al_{12}Mg_2Si$, Al_9Si. On the other hand, globular precipitates correspond to the so-called "β" phase and round ones to the "π" phase.

V. Conclusion

After conducting a study on the aging of cast aluminum alloy A356 and its effects on mechanical properties and microstructure, the following conclusions are drawn:

1. Natural and artificial aging hardness increase with increasing holding time. A longer holding time causes an increase in precipitated phases and / or intermetallic compounds; resulting in precipitation hardening.
2. In natural aging, the hardness is directly related to the quenching medium. The highest hardness values are found when the samples are cooled in dry ice (-40 °C); that is, the highest hardness values are found with the highest hardening rate.
3. The hardening effect at the beginning of the process is faster. In artificial aging, a notable increase in hardness is observed in the first 4 h.
4. The yield strength (YS) and the mechanical resistance (UTS) increase with the artificial aging time, and the elongation "ε" presents an oscillating or random behavior, due to the variation of precipitate cycles that the microstructure undergoes.
5. The maximum mechanical resistance UTS (300 MPa) goes together with an elongation of 5.3%, and is achieved with the maximum natural and artificial aging time (10 hr). The maximum ductility is ε = 11%, which is coupled with a mechanical resistance of 250 MPa, it is achieved with the maximum natural aging time (10h) and the minimum artificial aging time (2h). On the other hand, the modulus of elasticity (E) is almost constant and hardly alters with the aging heat treatment.
6. All microstructures show a matrix of the primary phase, composed of aluminum and Silicon surrounded by eutectic structures with various types of precipitates and / or intermetallic compounds, with different morphology and composition. Probably: Mg_2Si, $Al_{12}Mg_2Si$, Al_9Si

References

[1]. Jambor, M. Beyer, New cars – New Material, Technical Report, Materials & Design, 18 (1997), pp. 203-209
[2]. Wang Q.G, Microstructural Effects on the Tensile and Fracture Behaviour of aluminium Casting Alloys A356/357, Metallurgical and Materials Transactions A, Volume 34A
[3]. Ouellet P., Samuel F.H., Investigation study of 356 and 319 Al alloys., *J.* Mater. Sci. 34 (1999) 4671–4697.
[4]. Crepeau, P.N., Antolovich S.D., Worden J.A., AFS Trans. 98 (1990) 813–822.
[5]. Wang, Y., Neff, D., Schwam, D. et al. Optimization of Permanent Mold Mechanical Property Test Bars in A356 Alloy Using a New Mold Design. Inter Metalcast 7, 25–38 (2013).
[6]. Fracasso F., Influence of quench rate on the hardness obtained after artificial ageing of an Al-Si-Mg alloy; Trabajo de tesis ejecutado en el área de materiales y manufactura del Instituto tecnológico de Jönköping, Suecia, 2010.
[7]. Kacar, H., Atik, E., Meric, C.: Journal of Materials and Processing Technology Vol. 142 (2003), p. 762.
[8]. Kamp N., Gao N., Starink M.J., Sinclair I.,: Int. Journal of Fatigue Vol. 29 (2007), p. 869.
[9]. Garcia-Celis A.I., Colas R., S. Valtierra S., Proceedings of the First International Automotive Heat Treating Conference, Puerto Vallarta, Mexico, 13–15 July, 1998.
[10]. Ouellet P., Samuel F.H., Gloria D., Valtierra, Int. J. Cast Met. Res. 10 (1997) 67–78.
[11]. Jorstad J.L., Rasmussen W.M. and Zalensas D.L., "Aluminum cast technology, 2nd Edition. American Foundry Society, Des Plaines, IL, USA (200n 35-53.
[12]. Troeger, L.P. and Starke, E.A., "Microstructural and Mechanical Characterization of a Superplastic 6xxx Aluminum Alloy", Materials Science and Engineering, A277, 102-113, 2000.
[13]. Marshall G., "Microstructural Control during Processing of Aluminium Canning Alloys, Journal of Materials Science, 1996, pp. 217-222.
[14]. Es-Said O.S., Lee D., Pfost, W.D., Thompson D.L. Patterson M., Foyos J., Marloth, R. Eng. Fail. Anal. 9 (2002) 99–107.
[15]. Furui M., Kitamura T., Ishikawa T., Ikeno S., Saikawa S.,Sakai N., Mater. Trans. 52 (2011) 1163–1167.
[16]. Tavitas-Medrano F.J., Mohamed A, M., Gruzleski J.E., Samuel F,H,, Doty H.W., J. Mater. Sci. 45 (2010) 641–651.
[17]. Bai Y., Zhao H., Mater. Des. 31 (2010) 4237–4243.
[18]. Ji-hua P., Xiao-long T., Jian-ting H.E., X.U. De-ying, Trans. Nonferr. Met. Soc. China 21 (2011) 1950–1956.
[19]. E. Sjölander, S. Seifeddine, J. Mater. Process. Technol. 210 (2010) 1249–1259.
[20]. Serizawa A, Hirosawa S, Sato T. Three-dimensional atom probe characterization of nanocluster responsible for multistep aging behavior of an Al-Mg-Si alloy, Metallurgical and Materials Transaction A, 2008, 39: 243-251.
[21]. Ceschini l, Morri A, Effects of the delay between quenching and aging on hardness and tensile properties of A356 aluminum alloy, Journal of Materials Engineering and Performance, 2013, 22(1): 200-205.
[22]. Edwards G, Stiller K, Dunlop G, Couper M.. The precipitation sequence in Al-Mg-Si alloys. Acta Materialia, 1998, 46(11): 3893-3904.
[23]. Ravi c, Wolverton C. First-principles study of crystal structure and stability of Al-Mg-Si-(Cu) precipitates, Acta Materialia, 2004, 52: 4213-4227.
[24]. Hafenstein S., Werner E.., Direct aging of a hot isostatically pressed A356 aluminum cast alloy, Materials Science & Engineering A 768 (2019) 138417
[25]. Gwózdz M. Kwapisz K.., Influence of ageing process on the microstructure and mechanical properties of aluminium-silicon cast alloys - Al-9%Si-3%Cu and Al-9%Si-0.4%Mg, Bachelor Thesis, Jönköping University, Suecia, June 2008.
[26]. Ppreparacion de probetas para la observación microscópica. Available on page: https://chirinossilvaroger.files.wordpress.com/2015/10/metalografia_procedimiento.pdf
[27]. MacKenzie D.S., Quench rate effects on the natural aging behavior of 7xxx Al-Mg-Zn-Cu aluminum alloys, 18th Congress IFHTSE, July 26th - 30th, 2010 – Rio de Janeiro, Brazil
[28]. Kelly A., Nicholson R.B., Progress Mater. Sci. 10 (1963) 149.
[29]. Healey J.T.,Guinier-Preston Zone Evolution in 7075 Aluminum, Thesis to obtain of Doctor Degree , University of Florida, 1976.

[30]. Abdulwahab, M.; Madugu,.A.; Yaro, S.A.; Hassan, S.B.; Popoola, A.P.I. Effects of multiple-step thermal ageing treatment on the hardness characteristics of A356.0-type Al-Si-Mg alloy. Mater. Des. 2011, 32, 1159–1166.
[31]. Efecto de los Tratamientos Termicos en las Aleciones de Aluminio., Available on page:
[32]. https://upcommons.upc.edu/bitstream/handle/2117/93359/07Mtbp07de29.pdf?sequence=7&isAllowed=y
[33]. Tsao C.S., C.Y.Chen, and U.S.Jeng: Precipitation kinetics and transformation of metastable phases in Al–Mg–Si alloys; Acta Materialia Vol.54(2006), p.4
[34]. Wang G., Liu Y., Ren G. and Zhao Z., Analyzing Si precipitation on age hardening of an Al-Si-Mg cast alloy, (J) Advanced Materials Research Vols 146-147 (2011) pp 1685-1689

Victor Alcántara Alza. "Aging of Cast Aluminum Alloy A356: Effects on Mechanical Properties and Microstructure." *IOSR Journal of Mechanical and Civil Engineering (IOSR-JMCE)*, 18(6), 2021, pp. 54-65.